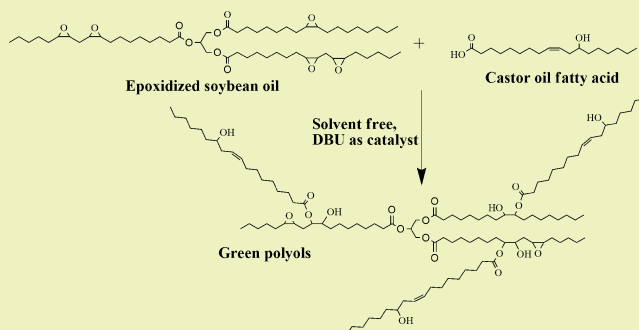


Polyurethanes from Solvent-Free Vegetable Oil-Based Polyols

Chaoqun Zhang,[†] Yuzhan Li,[†] Ruqi Chen,[†] and Michael R. Kessler^{*,†,‡}[†]Department of Materials Science and Engineering, Iowa State University, Ames, Iowa 50011, United States[‡]School of Mechanical and Materials Engineering, Washington State University, Pullman, Washington 99164, United States

ABSTRACT: The catalytic effects of 1,8-diazabicyclo[5.4.0]-undec-7-ene (DBU) and pyridine on the ring-opening reaction between epoxidized soybean oil and fatty acids from castor oil in a solvent free process were investigated using differential scanning calorimetry and were analyzed using both model-free and model-fitting methods. The resulting biopolyols from this reaction with epoxidized soybean oil, and similarly prepared polyols from epoxidized linseed oil, were characterized by proton nuclear magnetic resonance, Fourier transform infrared spectroscopy, and gel permeation chromatography. Polyurethane films were prepared by step-growth polymerization of the biopolyols with isophorone diisocyanate and were characterized by dynamic mechanical analysis, thermogravimetric analysis, and tensile tests. Polyurethanes from polyols manufactured with DBU as catalyst exhibited higher glass transition temperatures, tensile strength, and Young's modulus than polyurethanes from polyols manufactured using a catalyst-free method, which was attributed to the more homogeneous structure of their cross-linked network.

KEYWORDS: Epoxidized soybean oil, Differential scanning calorimetry, Reaction kinetics, Thermoset polymers, Activation energy, Renewable chemicals



INTRODUCTION

Polyurethanes, formed by step-growth polymerization of isocyanate with polyol, are an important class of polymers with an exceptionally versatile range of properties and applications.^{1,2} In order to meet specific requirements, their structure and properties can be tailored by the appropriate selection of polyol and polyisocyanate monomers. In industry, only a limited number of polyisocyanates are commonly used, while a variety of polyols are available.³ Therefore, the choice of polyol typically determines the properties of the created polyurethanes. Although recently much progress has been made in the development of new polyols for polyurethanes, most of the starting materials are petroleum-based, which causes environmental concerns and subjects the PUs to the large price fluctuations of crude oil.⁴

Vegetable oils are among the most promising options as feedstock for green polyols to produce PUs because they are readily available in large quantities, inherently sustainable, and available at relatively low cost.^{2,5} Vegetable oils are triglycerides consisting of glycerol and three fatty acids. The most common fatty acids are (1) saturated: palmitic (C16:0) and stearic (C18:0) and (2) unsaturated: oleic (C18:1), linoleic (C18:2), and linolenic (C18:3). [In this notation, the first number represents the number of carbon atoms in the fatty acid chain and the second number represents the number of carbon-carbon double bonds in the fatty acid.]

Some fatty acids have specific functional groups, such as hydroxyl-containing ricinoleic acid (C18:1-OH). Different vegetable oils have different compositions of fatty acids,

depending on the plant type and climatic conditions at harvest.⁶ Generally, the reactive sites within vegetable oils are esters and carbon-carbon double bonds, and these reactive sites can be utilized to introduce various other functional groups.

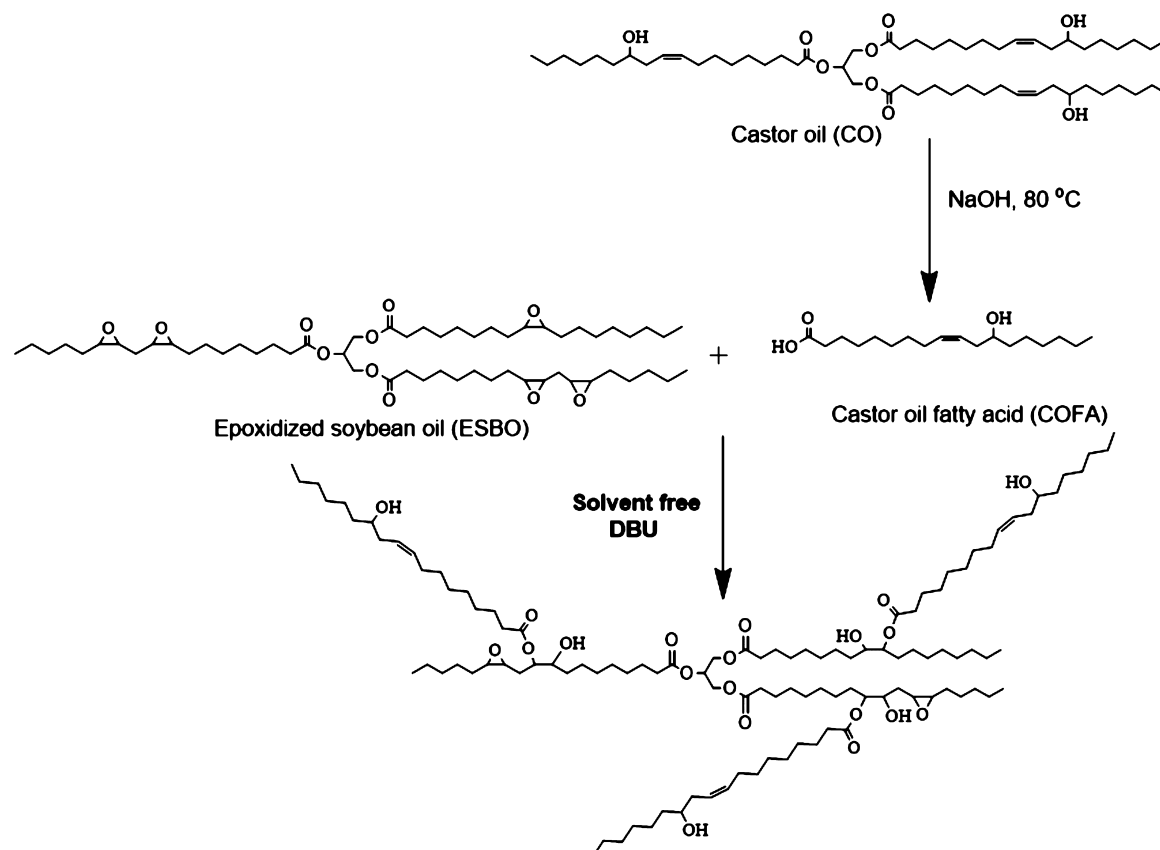
Epoxidation and subsequent oxirane ring opening is a common method to prepare polyols from vegetable oil using ring-opening agents, such as alcohols, inorganic acids, and hydrogenation for ring opening.⁷⁻¹¹ However, most ring-opening agents are derived from petroleum, and as a result, the resulting polyols are only partially composed of biorenewable precursors. Currently, several research groups dedicate considerable effort to the development of 100% biopolyols for PUs. For example, Kiatsimkul¹² prepared high hydroxyl equivalent weight polyols from epoxidized soybean oils that were ring opened by linoleic acid (LA), ricinoleic acid (RC), or ricinoleic acid estolide without catalysts. Our group developed polyols by ring opening of epoxidized soybean oil with castor oil fatty acid using a solvent/catalyst free method.¹³ However, the reactions were conducted at high temperatures (approximately 170 °C) and with long cycle times (approximately 8 h), which not only increased the cost of preparation but also promoted side reactions. One approach to overcome these issues is the use of catalysts for the ring-opening reaction. Several catalysts are frequently used to speed up epoxy-acid

Received: August 10, 2014

Revised: September 11, 2014

Published: September 15, 2014

Scheme 1. Preparation of Representative Polyols



reactions, such as bases (e.g., amine), onium compounds (e.g., triphenyl phosphine), metals (e.g., chromium compounds), and cationic catalyst (e.g., Lewis acids).¹⁴ Among them, amines have been widely investigated and show good catalytic effect in vegetable oil-based epoxy systems.^{9,15} Pan⁹ reported the use of 1,8-diazabicyclo[5.4.0]undec-7-ene (DBU) as a catalyst in polyol preparation from epoxidized sucrose esters of soybean oil ring opened by several organic acids. Matharu¹⁴ synthesized thermosetting resins from epoxidized linseed oil and bioderived diacid cross-linker with different amine catalysts and reported that 4-dimethylaminopyridine aided cross-linking between the epoxy and the carboxylic groups, followed by etherification. But few researchers systematically investigated the reaction kinetics of the ring-opening reaction between epoxidized vegetable oils and the ring-opening agents, and the effects of amine catalysts on the preparation of polyols for polyurethanes are still not fully understood.

In this paper, we report the effects of DBU and pyridine on the ring-opening reaction between epoxidized soybean oil and castor oil-based fatty acids using differential scanning calorimetry (DSC). Furthermore, biopolyols were prepared from ESBO and epoxidized linseed oil (ELO) using a solvent-free method with DBU as catalyst under mild reaction conditions. Moreover, polyurethanes were prepared from isophorone diisocyanate (IPDI) and biopolyols. The mechanical and thermal properties of these polyurethanes were compared with those of PUs from biopolyols manufactured using a catalyst-free method.

EXPERIMENTAL SECTION

Materials. Epoxidized soybean oil (ESBO), with approximately 4.3 oxirane rings per triglyceride, and epoxidized linseed oil (ELO), with approximately 6 oxirane rings per triglyceride, were purchased from Scientific Polymer Inc., New York, NY. Magnesium sulfate (MgSO_4) and methyl ethyl ketone (MEK) were purchased from Fisher Scientific Company (Fair Lawn, NJ). Castor oil, hydrochloric acid, sodium hydroxide, isophorone diisocyanate (IPDI), and 1,8-diazabicyclo[5.4.0]undec-7-ene (DBU) were obtained from Sigma-Aldrich (Milwaukee, WI). All materials were used as received without further purification.

Saponification of Castor Oil. Castor oil-based fatty acids (COFA) are prepared by saponification of castor oil.¹³ Briefly, castor oil saponification was conducted at 80 °C by heating with sodium hydroxide solution for 3 h. Then, the solution was neutralized by hydrochloric acid. Finally, COFA are obtained by purification of solution through washing with water, drying over MgSO_4 , and filtering. COFA consist of ricinoleic acid (87.7–90.4%) and some other acids, such as linolenic, linoleic, or oleic acid.

Preparation of Polyols Based on ESBO, ELO, and COFA with DBU as Catalyst. Two series of polyols were prepared from ESBO and ELO ring opened by COFA: Soy–castor oil-based polyols (SCP-D) and linseed–castor oil-based polyols (LCP-D). First, COFA and ESBO were weighed and mixed in a flask with a magnetic stirrer. Then, DBU (1 wt %) was added to the mixture. Finally, the mixture was stirred homogeneously and maintained at 130 °C in a protective atmosphere of nitrogen. The procedure was monitored at intervals of 0.5 h by ¹H NMR and was stopped when the residual epoxy groups remained stable for 1 h. Scheme 1 shows the preparation of representative green polyols. According to the ratios of carboxylic groups to epoxy groups and the vegetable oils used, these polyols were identified as SCP-D_0.3, SCP-D_0.5, SCP-D_0.7, SCP-D_0.9, LCP-D_0.5, and LCP-D_0.7 (where S = epoxidized soybean oil, C = COFA, L = epoxidized linseed oil, P = polyol, D = DBU). For

example, the sample designated SCP-D_0.7 was a polyol made with DBU catalyst from epoxidized soybean oil (ESBO) and ring opened with COFA, and the ratio of COFA to ESBO was determined such that there were 0.7 carboxylic acid groups in the COFA per epoxide group in the EBSO (Table 1).

Table 1. Reagent Table for Preparation of Various Polyols

	reagents	molar ratios of carboxylic acid and epoxy groups	catalyst
SCP-D_0.3	ESBO, COFA	0.3	DBU
SCP-D_0.5	ESBO, COFA	0.5	DBU
SCP-D_0.7	ESBO, COFA	0.7	DBU
SCP-D_0.9	ESBO, COFA	0.9	DBU
LCP-D_0.5	ELO, COFA	0.5	DBU
LCP-D_0.7	ELO, COFA	0.7	DBU
SCP_0.5	ESBO, COFA	0.5	none
SCP_0.9	ESBO, COFA	0.9	none

Preparation of Polyurethanes Using Polyols. The polyurethanes were prepared as follows. First, polyols, IPDI (5% molar excess) and MEK were mixed continuously and maintained at 70 °C for 3 h. An additional catalyst was not necessary because the DBU used in the ring-opening reaction could also act as a catalyst for the PU polymerization. Then, the solutions were poured into a glass mold (length × width: 100 mm × 50 mm) and kept in an oven at 80 °C overnight. Finally, the polyurethane films were removed from the mold and cut into specific dimensions for thermo-mechanical testing.

Characterization. ¹H NMR spectroscopic analysis of the monomers and final products were conducted with a Varian spectrometer (Palo Alto, CA) at 300 MHz. All measurements were made using CDCl₃ as the solvent. A Nicolet 460 FTIR spectrometer (Madison, WI) was used to record the FTIR spectra of monomers and polyols. The OH numbers of the polyols were determined using the Unilever method.¹⁶ The acid numbers of the polyols were determined according to AOCS Official Method Te 1a-64. The molecular weight was determined using a THF-eluted GPC equipped with a refractive index detector. The HPLC system used was a Thermo Scientific Dionex Ultimate 3000 (Sunnyvale, CA) equipped with a Shodex Refractive Index (RI). The eluent used was tetrahydrofuran with two

Agilent PL gel at 3 μm, 100 Å, and 300 mm × 7.5 mm (p/n PL1110-6320) and one mesopore at 300 mm × 7.5 mm (p/n PL1113-6325). The column flow rate and temperature was 1.0 mL/min at 25 °C.

A TA Instruments DMA Q800 dynamic mechanical analyzer in film-tension mode at 1 Hz was used to conduct dynamic mechanical analysis (DMA) of the PU films. Rectangular specimens of 0.6 mm × 10 mm (thickness × width) were used for the analysis. The samples were first cooled and held isothermally for 3 min at -40 °C and then heated to 150 °C at a rate of 5 °C/min. The glass transition temperatures (*T_g*) of the samples were obtained from the peaks of the tan δ curves.

Thermogravimetric analysis (TGA) of the films was carried out on a TA Instrument Q50 (New Castle, DE). The samples were heated from room temperature to 800 °C at a heating rate of 20 °C min⁻¹ in air. Generally, 10 mg samples were used for the TGA experiments.

A universal testing machine (Instron, model 4502) with a crosshead speed of 100 mm/min was used to determine the tensile properties of the polyurethane films. Rectangular specimens of 50 mm × 10 mm (length × width) were used. Average values of at least four replicates of each sample were taken.

RESULTS AND DISCUSSION

Effect of DBU Catalyst on Ring-Opening Reactions.

The DSC thermograms of the reactions between ESBO and COFA (with 1 wt % DBU/pyridine and without catalyst; molar ratios of carboxylic acid and epoxy = 0.5:1) are shown in Figure 1. For the formulations without catalyst, the thermograms showed two separate exothermic peaks at about 155 °C and above 170 °C (a broad peak), respectively. When pyridine was used as catalyst, both peaks shifted to a lower temperature, and the magnitude of the second peak reduced significantly. For the formulations catalyzed with DBU, the first peak continued to shift to lower temperatures, and the second peak almost disappeared (the two thermal events may still have been present but were beyond the resolution of the instrument).

The peak temperatures of formulations with pyridine and DBU are shown in Table 2. Matharu et al. studied the ring-opening reaction between epoxidized linseed oil and carboxyl

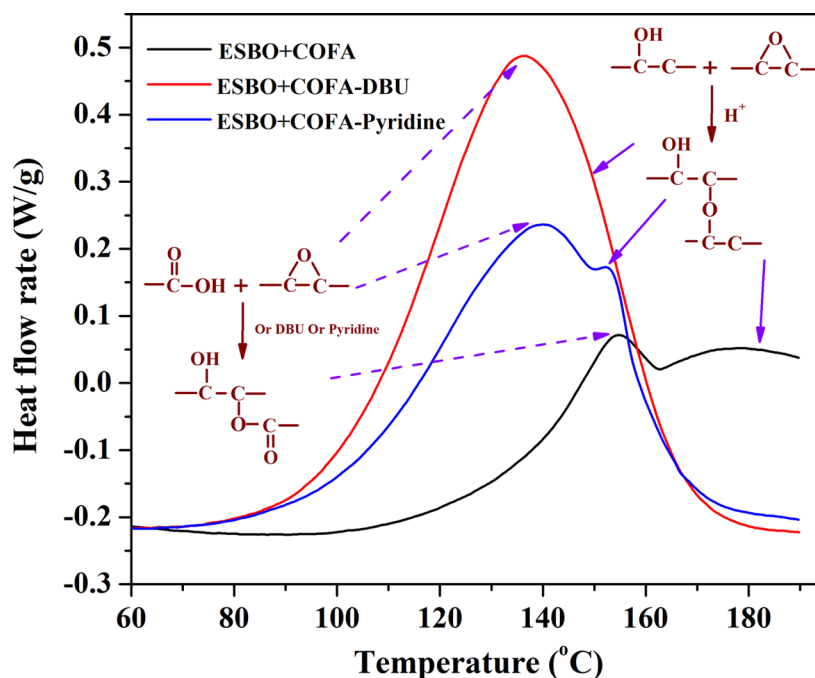


Figure 1. Thermograms of mixtures of ESBO and COFA with catalyst and without catalyst.

Table 2. DSC Analysis

catalyst	peak 1 temperature (°C)	peak 2 temperature (°C)
none	154.7	>170
pyridine	140.1	152.2
DBU	136.5	–

groups and reported that the first exothermic peak was related to the ring-opening reaction by the carboxyl groups, while the second thermal event corresponded to subsequent ring opening by the hydroxyl groups and cross-linking reactions.¹⁴ Thus, the DSC data indicates that use of DBU and pyridine reduced the reaction barrier and accelerated the reactions (first peak) while hindering the ring-opening reactions by the hydroxyl groups (second peak).

As reported earlier, both hydroxyl groups and carboxylic groups are involved in the ring-opening reaction, connecting two polyols together and leading to precross-linking of polyols in the formulations of ESBO and COFA without catalyst.¹³ Wu^{17,18} offered the following explanation for a possible hydroxyl group ring-opening mechanism. First, the catalyst protonates the oxygen atom in the oxirane group. An oxygen atom from a hydroxyl group then attacks one of the oxirane carbon atoms, and one hydroxyl atom attacks the oxirane oxygen atom. Finally, deprotonation regenerates the acid catalyst as shown in Scheme 2. When DBU and pyridine were used in the formulation, the concentration of free protons released by the carboxyl groups decreased because some of protons were attracted by the amine groups. Therefore, ring-opening reactions rates initiated by the hydroxyl groups decreased, resulting in less precross-linking of polyols (less oligomerization).¹⁹ Also, the reactions between carboxylate and epoxy groups increased due to the activation effect on carboxylic acid by amine as shown in Scheme 3. Because of the obvious catalyzing effect of DBU on reducing the reaction barrier and depression of oligomerization, reaction kinetics of the ring-opening reaction between ESBO and COFA catalyzed by DBU continued to be systematically studied by dynamic DSC as described below.

Reaction Kinetics of Ring-Opening Reactions with DBU as Catalyst. The effect of DBU on the reaction kinetics of the system was studied using dynamic DSC. The DSC measurements were performed at heating rates of 0.6, 0.8, 1.0, and 1.2 °C/min under a constant flow of helium at 25 mL/min. Data obtained were analyzed using Netzsch thermokinetics program (version 3.1). Both the model-free isoconversional method and the model-fitting method were used to extract the kinetic parameters.

In kinetic analysis, the rate of reaction can be described by eq 1

$$\frac{d\alpha}{dt} = k(T)f(\alpha) = A \exp\left(-\frac{E}{RT}\right)f(\alpha) \quad (1)$$

where α is the degree of conversion (ranging from 0 to 1), $k(T)$ is the temperature-dependent rate constant, and $f(\alpha)$ is the reaction model. Typically, $k(T)$ is described by the Arrhenius equation, in which R is the universal gas constant, E is the activation energy, and A is the pre-exponential factor. The heat flow dH/dt measured by DSC is directly related to the reaction rate by the following equation.²⁰

$$\frac{d\alpha}{dt} = \frac{dH/dt}{\Delta H} \quad (2)$$

For experiments carried out at a constant heating rate, eq 1 can be rearranged so that

$$\frac{d\alpha}{dT} = \frac{A}{\beta} \exp\left(-\frac{E}{RT}\right)f(\alpha) \quad (3)$$

where $\beta = dT/dt$ is the heating rate.

Model-Free Isoconversional Method. The model-free isoconversional method is well suited to describe the kinetics of complex reactions. It does not assume any definite form of a reaction model but rather allows for the variation of activation energy with conversion.²¹ The Friedman differential method is a commonly used isoconversional analysis method and can be derived by taking the logarithms of eq 1.

$$\ln\left(\frac{d\alpha}{dt}\right)_{\alpha,i} = \ln(A_{\alpha}f(\alpha)) - \frac{E_{\alpha}}{RT_{\alpha,i}} \quad (4)$$

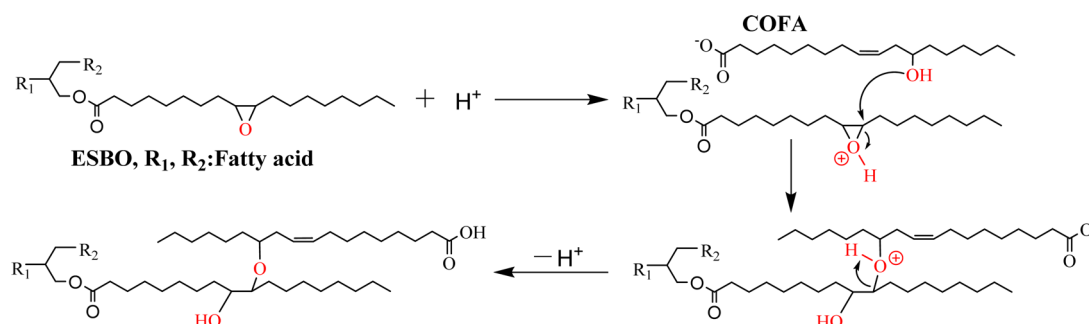
For a specific α at several heating rates β , the values of $(d\alpha/dt)_{\alpha,i}$ and $T_{\alpha,i}$ were determined from the DSC thermograms. The activation energy dependence of the conversion was then estimated from the plots of $\ln(d\alpha/dt)_{\alpha,i}$ vs $1/T_{\alpha,i}$ (Friedman plots). Kinetic information obtained through this isoconversional approach can then be used in the model-fitting method.

Model-Fitting Method. A multivariate model-fitting method is frequently used in the evaluation of dynamic DSC data so that the kinetic parameters (A and E) are obtained by a linearizing transformation of eq 3 as follows.²⁰

$$\ln \frac{d\alpha/dT}{f(\alpha)} = \ln\left(\frac{A}{\beta}\right) - \left(\frac{E}{RT}\right) \quad (5)$$

Different kinetic models can then be used to obtain the optimal fit of the kinetic parameters by multiple linear regressions. In addition, the Netzsch thermokinetics program allows fitting of a

Scheme 2. Mechanism of Ring-Opening Reactions between Epoxy and Hydroxyl Groups with Acid as Catalyst



Scheme 3. Mechanism of Ring-Opening Reactions between Epoxy and Carboxyl Acid Groups with Base as Catalyst

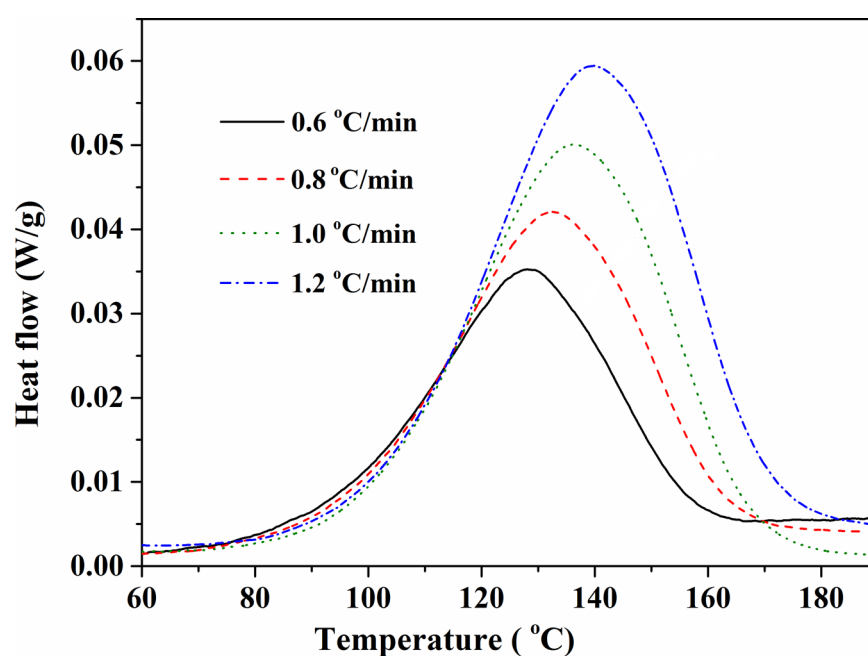
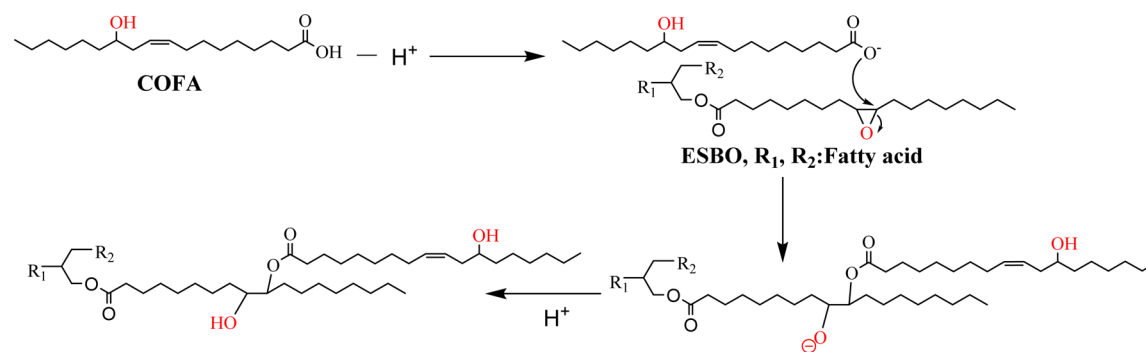


Figure 2. DSC dynamic scans at heating rates of 0.6, 0.8, 1, 1.2 °C/min.

multiple-step reaction, providing better simulation of the experimental results.

Figure 2 shows the dynamic DSC scans of the reacting system at different heating rates, and the total enthalpy of reaction is summarized in Table 3. The main peaks shifted to higher temperature regions with increasing heating rate.

Table 3. Total Enthalpy of Reaction at Different Heating Rates

heating rate (°C/min)	total enthalpy of reaction (J/g)
0.6	119.2
0.8	124.9
1	123.2
1.2	123.8

To estimate the activation energy for each step involved in the overall reaction, a Friedman plot was created. The conversion dependence of the activation energy was then determined from the Friedman plot. As shown in Figure 3, two processes with different activation energies were observed, possibly attributed to the reaction between epoxy groups and carboxylic groups and hydroxyl groups, respectively. The two reactions were considered independent, and both reactions

were simulated using an expanded Prout–Tompkins model,²² as shown in eq 6. Fitting results are shown in Figure 4, and kinetic parameters extracted from the model are summarized in Table 4.

$$f(a) = (1 - a)^n a^m \quad (6)$$

The model curves fit the experimental data very well over the entire temperature range. Table 4 shows that the activation energy for the ring-opening reaction between carboxylic acid and epoxy groups was 72.2 kJ/mol, while for the ring-opening reaction between the hydroxyl groups and the epoxy groups was 75.1 kJ/mol. Erhan²³ reported that the Arrhenius activation energy between propionic acid and epoxidation of methyl oleate under pseudo-first order conditions was 66.7 kJ/mol. Activation energy by *ab initio* calculation was 60.7 kJ/mol for the ring opening of an epoxide through an inversion transition state.²⁴ The activation energy values obtained by our study were higher than those reported; however, this was attributed to the fact that the molecules in our system had longer carbon chains than those used in the literature. Also, steric and electronics effects between epoxy groups in the same chain correspond to the higher activation energy. The activation energy of the ring-opening reaction between hydroxyl groups and epoxy groups with weak acid catalyst were 75.1 kJ/mol, a

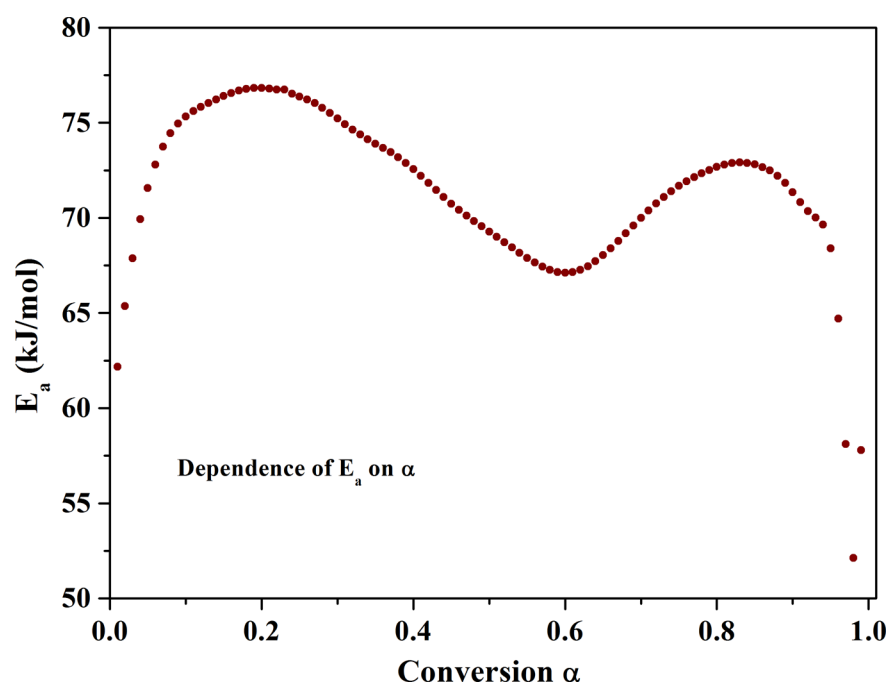


Figure 3. Activation energy dependence of conversion determined by Friedman analysis.

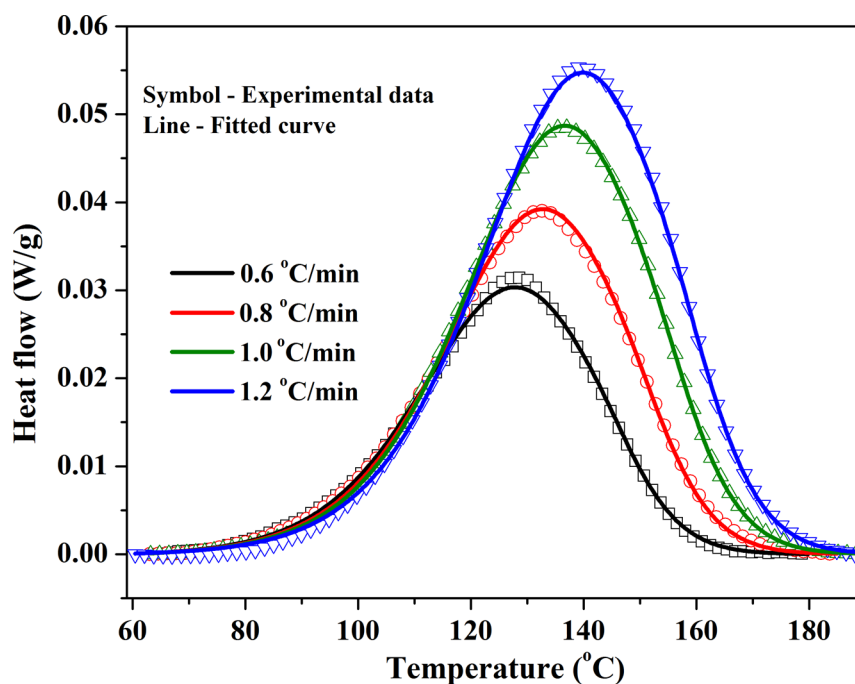


Figure 4. Model fits of DSC data.

Table 4. Results of Multiple Linear Regression Analysis

	process 1	process 2
model designation	$f(\alpha) = (1 - \alpha)^n \alpha^m$	$f(\alpha) = (1 - \alpha)^n \alpha^m$
$\log [A]$ (s^{-1})	6.333	6.634
E (kJ/mol)	72.218	75.083
N	1.166	1.139
M	0.267	0.651
correlation coefficient	0.999777	0.999777

little higher than that between carboxylic acid and epoxy groups.

Preparation and Characterization of Polyols with DBU as Catalyst.

Polyols were prepared from epoxidized soybean oils, ring opened by COFA. To confirm the catalyzing effect of DBU in the ring-opening reaction, polyols from epoxidized linseed oils were also prepared. As shown in Table 2, the peak temperature corresponding to the ring-opening reaction by carboxylic groups for formulations with DBU as catalyst was measured as 136.5 °C. Therefore, a temperature of 130 °C was chosen to prepare polyols with different ratios of carboxylic to epoxy groups. Scheme 1 showed the preparation of representative green polyols. The properties of the polyols were characterized by proton nuclear magnetic resonance (^1H

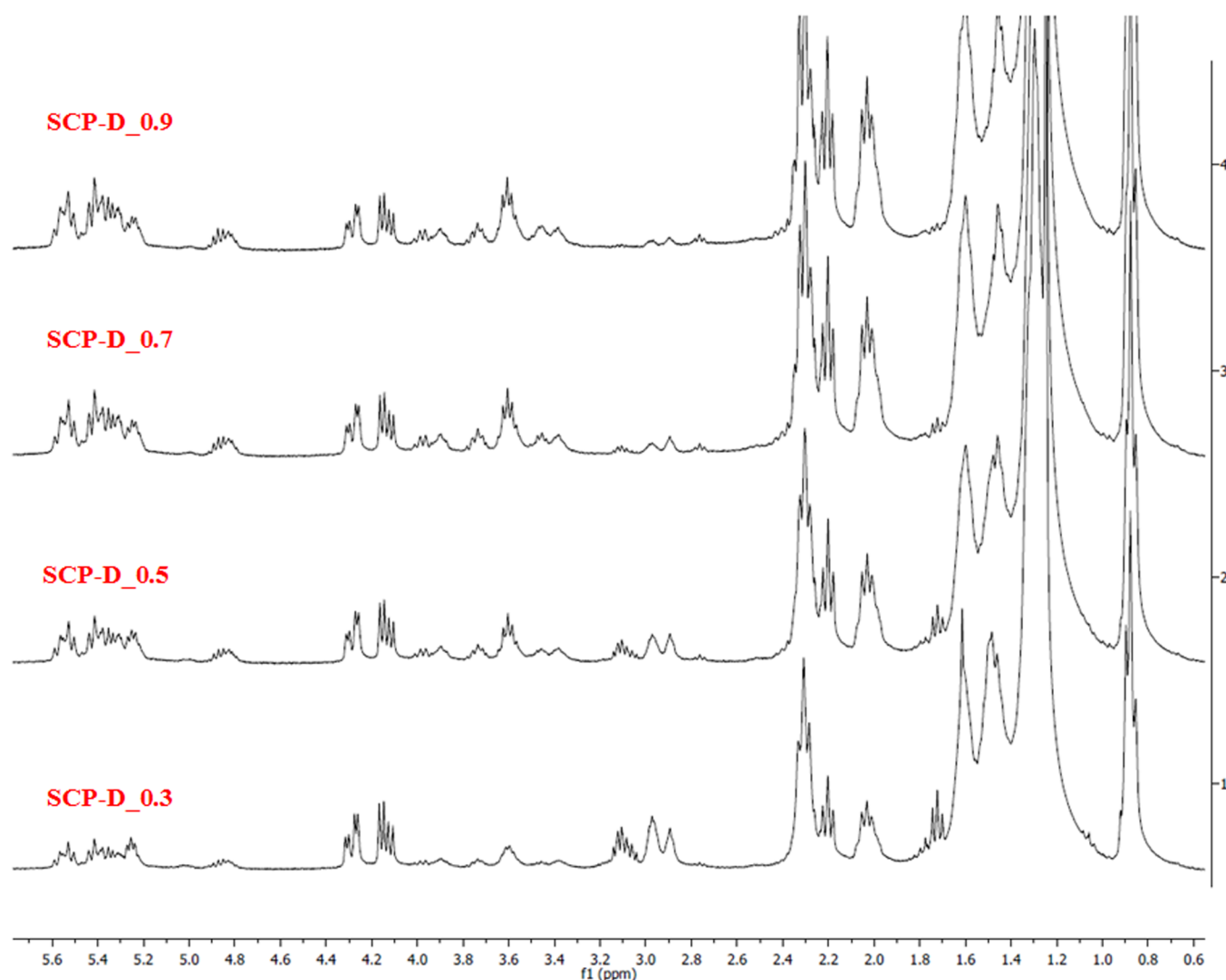


Figure 5. ^1H NMR spectra of SCP-D with different ratios of carboxyl to epoxy groups.

NMR), Fourier transform infrared spectroscopy (FTIR), and gel permeation chromatography (GPC).

Figures 5 and 6 show the NMR spectra of polyols prepared from epoxidized soybean oil and epoxidized linseed oil, ring opened by COFA using DBU as catalyst. It is shown that as the content of COFA increased the residual epoxy groups (represented by the peaks between 2.8 and 3.2 ppm) in SCP-D and LCP-D both decreased. The presence of new peaks between 4.6 and 5.0 ppm, representing tertiary hydrogen atoms adjacent to the newly formed ester groups, indicated that COFA was attached to the long carbon chain of the epoxidized oils. The peaks at 3.7–4.0 ppm correspond to hydrogen attached to the carbon adjacent to OH and hydrogen bonded to carbons adjacent to the ether. As the content of COFA increased, the peaks at 5.3–5.6 ppm (corresponding to carbon–carbon double bonds in COFA) increased, indicating that more COFA chains were attached to the long carbon chain of the epoxidized oils. The time needed to complete the reaction is shown in Table 5. It is shown that as the content of COFA increased longer time was needed to complete the reaction because of the increasing steric effect of the long chains in the structure of the polyols, which may hinder the accessibility of the acid groups as more COFA was attached to

the long chains. However, the time needed to complete the reaction with DBU as catalyst was shorter than the time needed without catalyst, indicating that DBU reduced the reaction time. Furthermore, the value of the integrated area for the peaks at 4.1–4.2 ppm ($-\text{CH}_2-\text{CHCH}_2-$) was used as an internal standard (assigned a constant integration area of 2.0) for normalization. The residual epoxy groups and carbon–carbon double bonds for different polyols are listed in Table 5.

Figure 7 shows the FTIR spectra of polyols prepared by COFA oxirane ring opening of ESBO and ELO. Oxirane absorption at 823 cm^{-1} corresponded to epoxy groups, while a broad peak at 3392 cm^{-1} indicated the presence of hydroxyl groups.²⁵ The disappearance of epoxy groups in the polyols indicated that the epoxy groups in ESBO were ring opened. A band at 1648 cm^{-1} was observed in the DBU system, corresponding to protonated amine,^{26,27} which confirmed the earlier conclusion that the amine group attracted the protons released by the carboxyl groups.

The GPC curves of SCP-D with different ratios of carboxyl to epoxy groups are shown in Figure 8. It is shown that as reaction ratios of carboxylic to epoxy groups increased in polyols prepared from ESBO, the main peak of the polyols shifted to lower retention times, indicating increased molecular

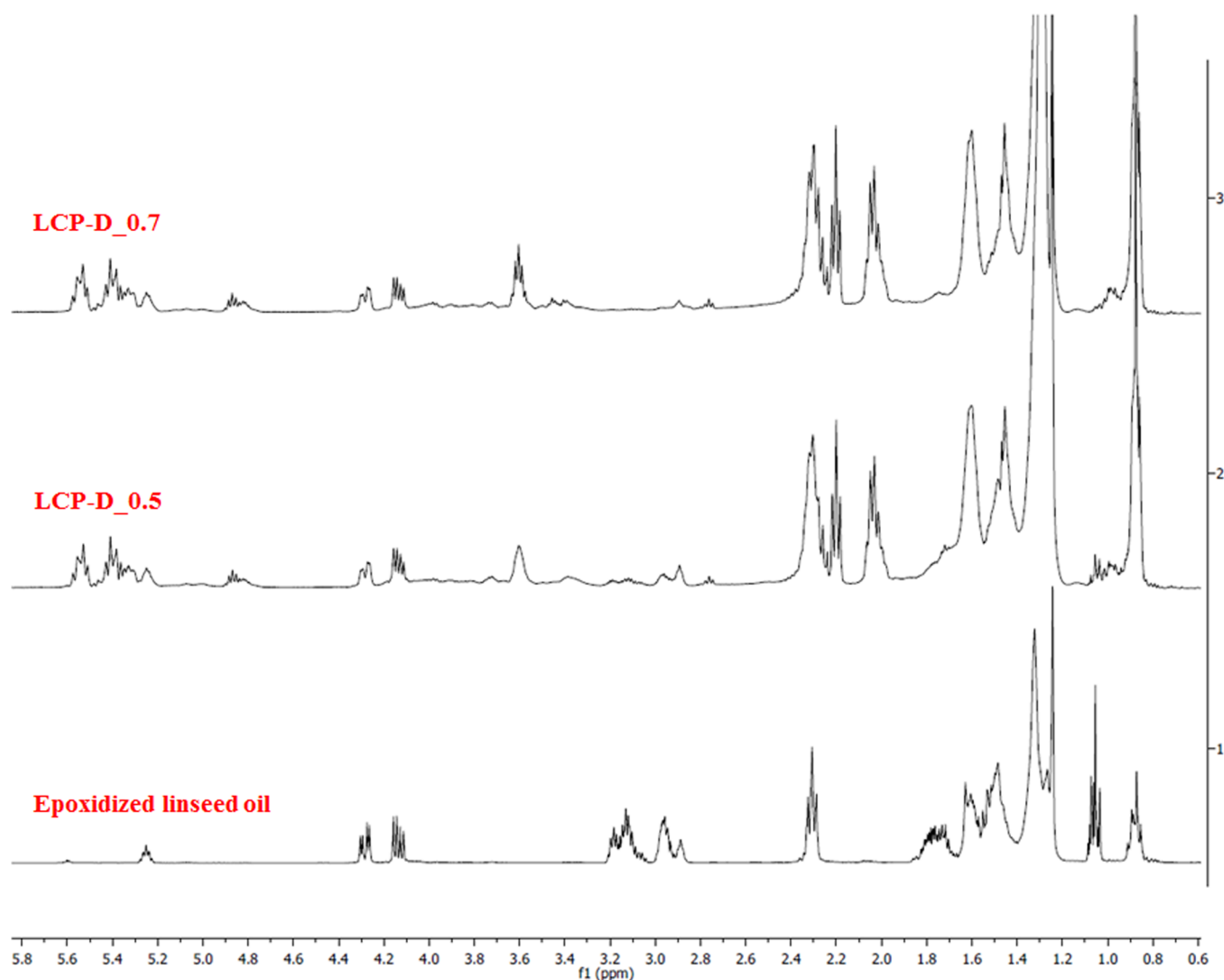


Figure 6. ^1H NMR spectra of LCP-D with different ratios of carboxyl to epoxy groups.

Table 5. Properties of SCP-D and LCP-D

	reaction time (h)	C=C bonds ^b	epoxy ^b	number-average Mw ^c	weight-average Mw ^c	PDI ^a	acid number (mg KOH/g)	titrated OH number (mg KOH/g)
SCP-D_0.3	5	1.632	2.929	2033	2358	1.16	0.5	124.1
SCP-D_0.5	5	2.756	1.624	2411	2780	1.15	3.3	140.9
SCP-D_0.7	6.5	3.473	0.988	2255	2944	1.31	10.2	150.9
SCP-D_0.9	6.5	4.672	0.029	1960	2879	1.47	22.0	157.61
LCP-D_0.5	6.5	3.0835	1.545	2799	3358	1.2	0.8	176.72
LCP-D_0.7	6.5	4.4425	1.292	2679	3615	1.35	9.2	183.84

^aPolydispersity index. ^bNumbers of functional groups per molecule by NMR. ^cMolecular weight.

weight. Compared to SCP_0.5–130 and SCP_0.9–170, which were prepared without catalyst at 130 and 170 °C,¹³ respectively, SCP-D_0.5–130 and SCP-D_0.9–170 contained less residual COFA, as shown in the peak at a retention time of 23 min, indicating that more COFA was attached to the long chains of epoxidized oils in the presence of a DBU catalyst. The GPC curve of SCP-D_0.9 indicated a narrow molecular weight distribution without the oligomerization peak (at a retention time of 16–17 min) seen for SCP_0.9–170. This can be explained by the fact that DBU hinders ring opening by hydroxyl groups, leading to less connection of polyols and less

oligomerization. The molecular weights of the polyols are listed in Table 5.

Polyurethane from SCP-D and LCP-D. SCP-D_0.3, SCP-D_0.5, SCP-D_0.7, and LCP-D_0.7 were chosen to prepare PU films, and their properties were characterized by DMA, TGA, and tensile strength tests. Because the PU from SCP-D_0.3 was so soft, it was difficult to collect mechanical data. It is worth noting that the ring-opening reaction and the subsequent polymerization reactions shared the same catalyst, namely, DBU. Thus, it is not necessary to remove the catalyst between the two steps, making this approach both time- and cost-effective.

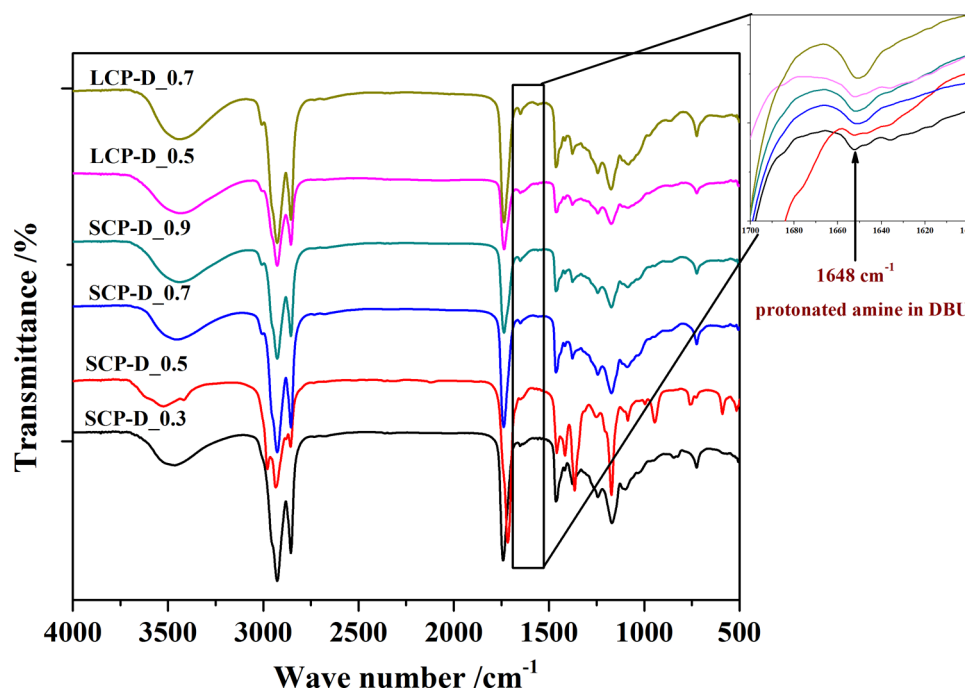


Figure 7. FTIR spectra of SCP-D and LCP-D with different ratios of carboxyl to epoxy groups.

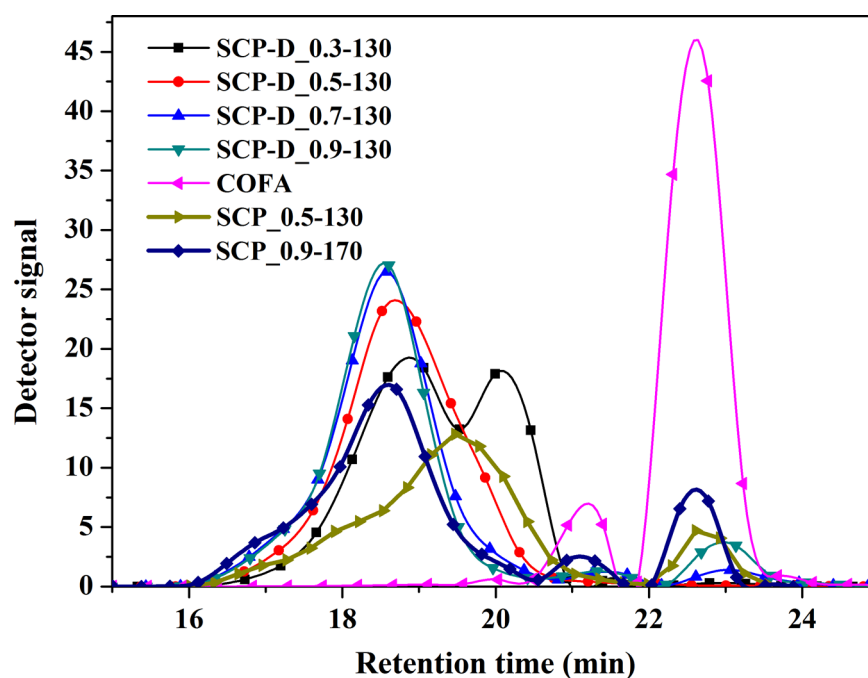


Figure 8. GPC curves of SCP-D with different ratios of carboxyl to epoxy groups.

Figure 9 shows storage modulus and loss factor as functions of temperature for PU films in the temperature range from -50 to 150 °C. With increasing temperature, all films showed a similar trend. In detail, with temperature increasing from -35 °C, E' slightly decreased, and once -10 °C was reached, a rapid decrease in E' was observed. A rubbery plateau for the storage modulus was observed in every curve in the higher temperature range of the tests, and a peak maximum was observed in the $\tan \delta$ versus temperature curves (α relaxation), which was taken as the glass transition temperature (T_g). All films show one $\tan \delta$ peak, indicating the homogeneous nature of the polyurethane

films. As the cross-linking densities increased, the molecular motion of the polymer chains became more restricted, and the amount of energy dissipated throughout the polymer decreased dramatically. Therefore, the $\tan \delta$ peak shifted to higher temperatures.^{8,28} As the OH number increased, cross-linking density increased, leading to a higher T_g and higher storage modulus. Compared with PUs from SCP_0.5, PUs from SCP-D_0.5 had a higher biocontent but a lower T_g as shown in Table 6. However, PUs from SCP-D_0.7 had a higher biocontent and a higher T_g .

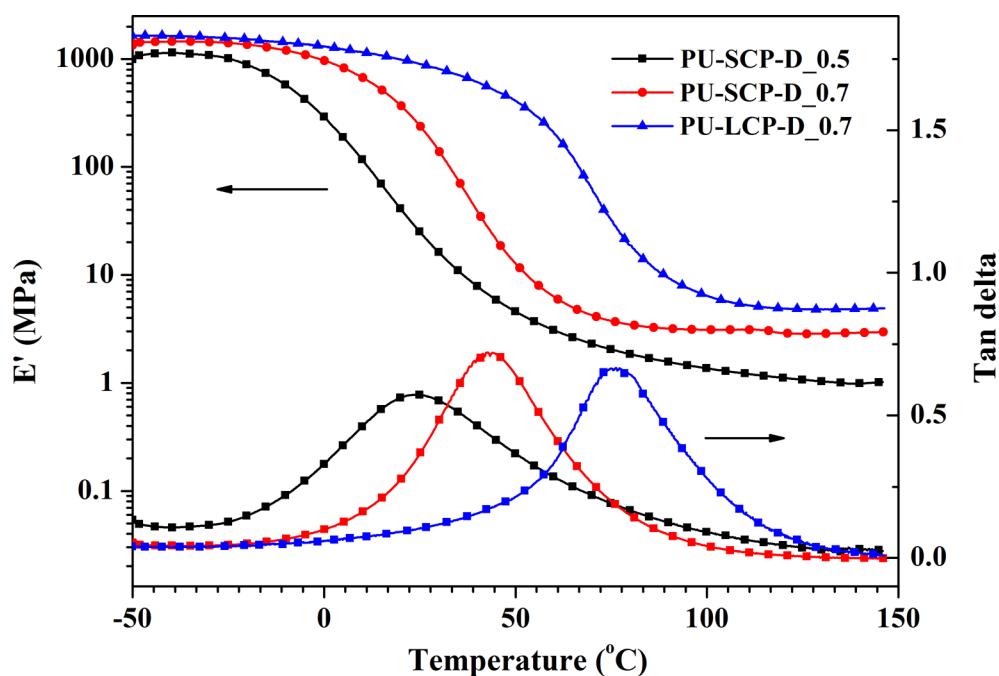


Figure 9. Storage modulus and loss factor as functions of temperature for PU films based on SCP-D and LCP-D.

Table 6. Thermal and Mechanical Properties of PUs Based on SCP-D_0.3, SCP-D_0.5, SCP-D_0.7, and LCP-D_0.7

	DMA T_g (°C)	TGA in air (°C)		tensile strength (MPa)	Young's modulus (MPa)	elongation at break (%)	biocontent (%)
		T_{10}	T_{50}				
PU-SCP-D_0.3	—	324	385	—	—	—	80
PU-SCP-D_0.5	24.0	318	374	3.5 ± 1.1	5.6 ± 1.1	107.0 ± 4.1	76
PU-SCP-D_0.7	42.5	318	372	12.4 ± 0.5	36.9 ± 5.6	157.3 ± 13.6	75
PU-LCP-D_0.7	69.0	314	370	20.1 ± 2.1	303.7 ± 45.7	104.0 ± 5.0	71
PU-SCP_0.5 ¹³	31.3	302	373	11.6 ± 0.4	5.8 ± 0.5	232.7 ± 18.0	72

Figure 10 shows TGA weight loss and weight loss derivative curves in air for the polyurethane films. The degradation of the polyurethanes observed at temperatures between 200 and 350 °C was attributed to the decomposition of labile urethane groups. The degradation observed in the temperature range from 350 to 500 °C resulted from chain scission in the soybean oil. The last degradation step above 500 °C corresponded to further thermo-oxidation of the PU films in air. In the first decomposition stage, as the COFA content increased leading to higher OH numbers, the thermal stability of the PU films from SCP-D and LCP-D decreased as a result of the higher number of urethane bonds. PUs from SCP_0.5 had more urethane bonds and therefore exhibited lower thermal stability than PU from SCP-D. In the second and third degradation stage as the COFA content increased, the thermal stability of PU from SCP-D and LCP-D decreased because the thermal resistance of COFA is lower compared to that of ESBO. PUs from SCP_0.5 exhibited higher thermal resistance than PUs from SCP-D and LCP-D because of the cross-linking of the polyols. Table 6 shows that 10% degradation (T_{10}) occurred at 302, 324, 318, 318, and 314 °C, respectively, for the five PUs investigated, and 50% degradation (T_{50}) was detected at 373, 385, 374, 372, and 370 °C, respectively.

Table 6 summarizes the Young's moduli, tensile strength, elongation at break, and biocontent of the polyurethane films investigated. PUs based on LCP-D_0.7 exhibited the highest tensile strength (20.1 MPa) and a higher Young's modulus

(303.7 MPa) compared to other PU films because of their higher cross-linking density. Although PUs from SCP-D_0.5 exhibited lower tensile strength and Young's moduli than PUs from SCP_0.5 because of their lower cross-linking density, they had a higher biocontent. PUs from SCP-D_0.7 exhibited higher tensile strength, Young's moduli, and biocontent than PUs from SCP_0.5. The oligomerization structure of SCP compromised the polyurethanes' tensile strength. However, polyurethanes based on SCP-D and LCP-D exhibited a lower value for elongation at break compared to PUs based on SCP

CONCLUSION

DBU not only reduced the barrier for ring-opening reactions between epoxidized vegetable oils and COFA, resulting in a decrease in reaction temperature and reaction time, but also hindered the epoxy ring-opening reaction by the hydroxyl group, leading to less oligomerization and a more homogeneous structure of the polyols. The activation energy of the ring-opening reaction between the epoxy and carboxylic groups with DBU as catalyst was 72.2 kJ/mol, while the activation energy of the ring-opening reaction between epoxy and hydroxyl groups with protons as catalysts was 75.1 kJ/mol. The homogeneous structure of the polyols had a positive effect on the properties of the final polyurethanes, such as higher T_g and higher Young's modulus.

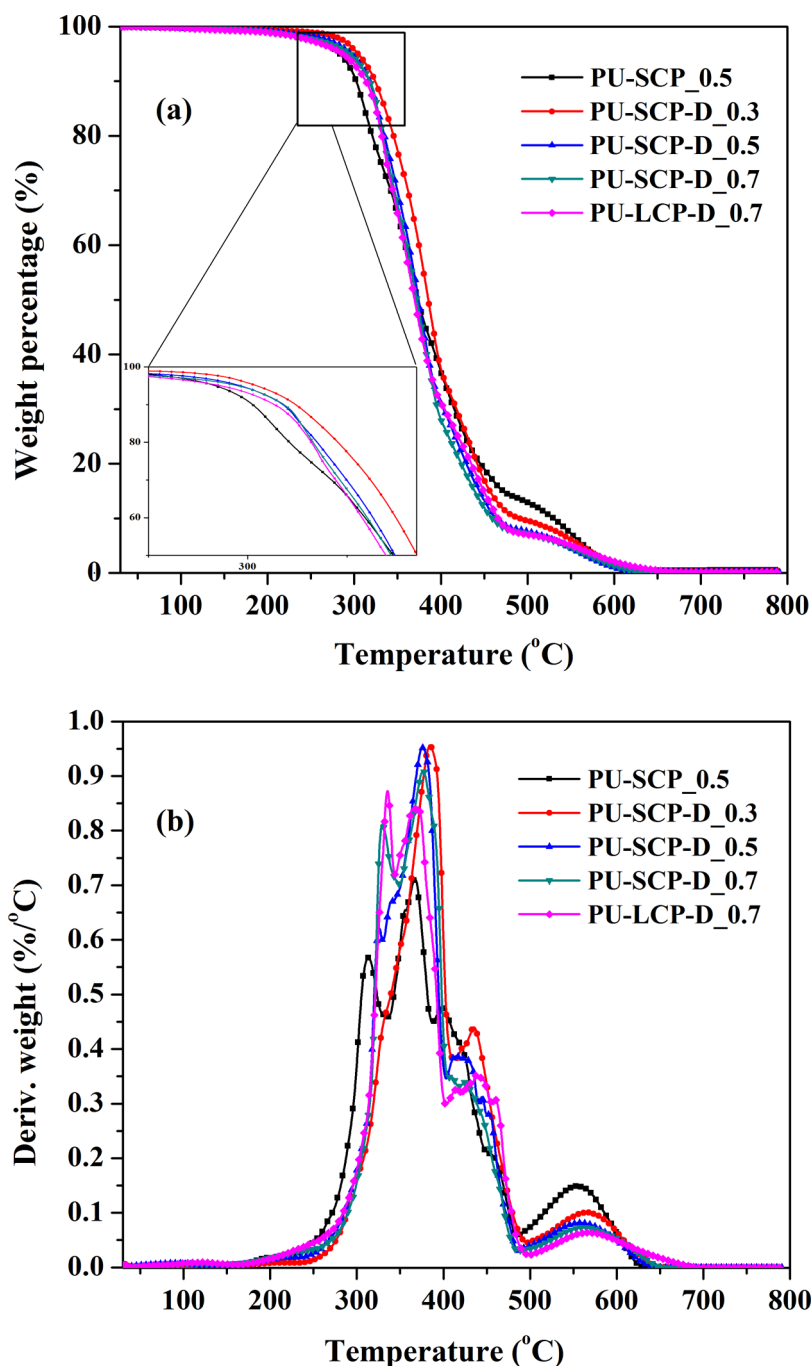


Figure 10. TGA curves (a) and their derivative curves (b) for PU films based on SCP, SCP-D, and LCP-D.

AUTHOR INFORMATION

Corresponding Author

*E-mail: MichaelR.Kessler@wsu.edu.

Notes

The authors declare no competing financial interest.

ACKNOWLEDGMENTS

GPC Analysis by Patrick A. Johnston at the Center for Sustainable Environmental Technologies, Iowa State University, is gratefully acknowledged.

REFERENCES

- (1) Lligadas, G.; Ronda, J. C.; Galia, M.; Cadiz, V. Poly(ether urethane) networks from renewable resources as candidate biomaterials: Synthesis and characterization. *Biomacromolecules* **2007**, *8*, 686–692.
- (2) Xia, Y.; Larock, R. C. Vegetable oil-based polymeric materials: Synthesis, properties, and applications. *Green Chem.* **2010**, *12*, 1893–1909.
- (3) Pfister, D. P.; Xia, Y.; Larock, R. C. Recent advances in vegetable oil-based polyurethanes. *ChemSusChem* **2011**, *4*, 703–717.
- (4) Petrovic, Z. S. Polyurethanes from vegetable oils. *Polym. Rev.* **2008**, *48*, 109–155.
- (5) Williams, C. K.; Hillmyer, M. A. Polymers from renewable resources: A perspective for a special issue of polymer reviews. *Polym. Rev.* **2008**, *48*, 1–10.

- (6) Meier, M. A. R.; Metzger, J. O.; Schubert, U. S. Plant oil renewable resources as green alternatives in polymer science. *Chem. Soc. Rev.* **2007**, *36*, 1788–1802.
- (7) Guo, A.; Cho, Y. J.; Petrovic, Z. S. Structure and properties of halogenated and nonhalogenated soy-based polyols. *J. Polym. Sci., Part A: Polym. Chem.* **2000**, *38*, 3900–3910.
- (8) Petrovic, Z. S.; Zhang, W.; Zlatanic, A.; Lava, C. C. Effect of OH/NCO molar ratio on properties of soy-based polyurethane networks. *Abstr Pap Am. Chem. S* **2002**, *223*, D95–D95.
- (9) Pan, X.; Webster, D. C. New biobased high functionality polyols and their use in polyurethane coatings. *ChemSusChem* **2012**, *5*, 419–429.
- (10) Wang, C. S.; Yang, L. T.; Ni, B. L.; Shi, G. Polyurethane networks from different soy-based polyols by the ring opening of epoxidized soybean oil with methanol, glycol, and 1,2-propanediol. *J. Appl. Polym. Sci.* **2009**, *114*, 125–131.
- (11) Petrovic, Z. S.; Guo, A.; Zhang, W. Structure and properties of polyurethanes based on halogenated and nonhalogenated soy-polyols. *J. Polym. Sci., Part A: Polym. Chem.* **2000**, *38*, 4062–4069.
- (12) Kiatsimkul, P. P.; Suppes, G. J.; Hsieh, F. H.; Lozada, Z.; Tu, Y. C. Preparation of high hydroxyl equivalent weight polyols from vegetable oils. *Ind. Crop Prod* **2008**, *27*, 257–264.
- (13) Zhang, C. Q.; Xia, Y.; Chen, R. Q.; Huh, S.; Johnston, P. A.; Kessler, M. R. Soy-castor oil based polyols prepared using a solvent-free and catalyst-free method and polyurethanes therefrom. *Green Chem.* **2013**, *15*, 1477–1484.
- (14) Supanchaiyamat, N.; Shuttleworth, P. S.; Hunt, A. J.; Clark, J. H.; Matharu, A. S. Thermosetting resin based on epoxidised linseed oil and bio-derived crosslinker. *Green Chem.* **2012**, *14*, 1759–1765.
- (15) Blank, W. J.; He, Z. A.; Picci, M. Catalysis of the epoxy-carboxyl reaction. *J. Coating Technol.* **2002**, *74*, 33–41.
- (16) Phaneuf, M. D.; Bide, M. J.; Szycher, M.; Gale, M. B.; Huang, H. X.; Yang, C. Q.; LoGerfo, F. W.; Quist, W. C. Development of infection resistant polyurethane biomaterials using textile dyeing technology. *Asaio J.* **2001**, *47*, 634–640.
- (17) Wu, S. B.; Soucek, M. D. Mechanism of oligomerization for cyclohexene oxide. *Abstr. Pap. Am. Chem. Soc.* **1996**, *212*, 108.
- (18) Wu, S. B.; Soucek, M. D. Oligomerization mechanism of cyclohexene oxide. *Polymer* **1998**, *39*, 3583–3586.
- (19) Xu, Y. J.; Petrovic, Z. S. Comments on the paper: Kinetics studies on oxirane cleavage of epoxidized soybean oil by methanol and characterization of polyols. *J. Am. Oil Chem. Soc.* **2008**, *85*, 1185–1186.
- (20) Kessler, M. R.; White, S. R. Cure kinetics of the ring-opening metathesis polymerization of dicyclopentadiene. *J. Polym. Sci., Part A: Polym. Chem.* **2002**, *40*, 2373–2383.
- (21) Vyazovkin, S.; Sbirrazzuoli, N. Isoconversional kinetic analysis of thermally stimulated processes in polymers. *Macromol. Rapid Commun.* **2006**, *27*, 1515–1532.
- (22) Opfermann, J. R.; Kaisersberger, E.; Flammersheim, H. J. Model-free analysis of thermoanalytical data-advantages and limitations. *Thermochim. Acta* **2002**, *391*, 119–127.
- (23) Doll, K. M.; Sharma, B. K.; Erhan, S. Z. Synthesis of branched methyl hydroxy stearates including an ester from bio-based levulinic acid. *Ind. Eng. Chem. Res.* **2007**, *46*, 3513–3519.
- (24) Harder, S.; Vanlenthe, J. H.; Hommes, N. J. R. V.; Schleyer, P. V. Nucleophilic ring-opening of epoxides by organolithium compounds: Ab-initio mechanisms. *J. Am. Chem. Soc.* **1994**, *116*, 2508–2514.
- (25) Adhvaryu, A.; Erhan, S. Z. Epoxidized soybean oil as a potential source of high-temperature lubricants. *Ind. Crops Prod.* **2002**, *15*, 247–254.
- (26) Heldebrant, D. J.; Jessop, P. G.; Thomas, C. A.; Eckert, C. A.; Liotta, C. L. The reaction of 1,8-diazabicyclo[5.4.0]undec-7-ene (DBU) with carbon dioxide. *J. Org. Chem.* **2005**, *70*, 5335–5338.
- (27) Huczynski, A.; Ratajczak-Sitarz, M.; Katrusiak, A.; Brzezinski, B. Cocrystals of Kemp's triacid. Part I: Molecular structure of 2:2 complex of 1,5,7-triazabicyclo[4.4.0]dec-5-ene with Kemp's triacid. *J. Mol. Struct.* **2008**, *888*, 84–91.
- (28) Xia, Y.; Larock, R. C. Castor-oil-based waterborne polyurethane dispersions cured with an aziridine-based crosslinker. *Macromol. Mater. Eng.* **2011**, *296*, 703–709.